IEEE Access
Multidisciplinary | Rapid Review | Open Access Journal

SPECIAL SECTION ON COLLABORATION FOR INTERNET OF THINGS

Received July 2, 2018, accepted August 1, 2018, date of publication August 10, 2018, date of current version September 5, 2018.

Digital Object Identifier 10.1109/ACCESS.2018.2864611

Application of Time-Difference-of-Arrival Localization Method in Impulse System Radar and the Prospect of Application of Impulse System Radar in the Internet of Things

LONGFEI DANG, HONGCHUN YANG, AND BAOHUA TENG
School of Physics, University of Electronic Science and Technology of China, Chengdu 610054, China
Corresponding author: Longfei Dang (lfdang@163.com)

ABSTRACT The impulse system radar is based on the generation, transmission, radiation, receiving, data collection, data processing, and imaging of impulse signals. It identifies the position or shape of the target object by accurately measuring the time difference and the waveform parameter difference of the electromagnetic signals reflected by the target object. It is a typical impulse-system-based ultra-wideband radar. Based on the existing studies on transmission characteristics of impulse signals and radiation characteristics of elementary time-domain antennas, a ''point source approximation'' analytical model, which considers an elementary antenna as the radiation point source and can reflect the radiation characteristics of specific elementary antennas, is proposed. On this basis, a time-difference-of-arrival (TDOA) method, whereby targets are localized by testing the TDOA of non-collinear multi-antenna (three or more) for target echo signaling, is proposed. Meanwhile, a detailed analytical analysis and numerical calculation programming are performed. Experimental test results show that the present method enables fairly accurate localization of targets. The application of time-difference localization in an impulse radar can also be extended to the Internet of Things. Positioning and tracking targets by an impulse radar is exactly a key technology in the application of Internet of Things. The research work done in this paper has excellent application values in Internet of Things.

INDEX TERMS Impulse signal, Internet of Things, point source approximation, time-difference-of arrival(TDOA) method, time domain antenna.

I. INTRODUCTION

Impulse radar is highly valuable to engineering design and development of high-tech military, civil radar, and other systems (including four-resistance radar, wall or ground penetrating radar, jungle radar, precision guidance radar, time-domain proximity fuse, borehole well-logging radar, and geological disaster monitoring radar). Over the last two decades, researchers wordwide have conducted extensive studies on photoconductive switch-based impulse radar [1]–[2]. Compared to continuous wave radar, impulse radar has many advantages, such as a simple structure, low interception, high resolution, electromagnetic interference resistance, and a strong anti-stealth ability. Although theoretical studies have been conducted on energy transmission characteristics, beam focusing, beam scanning characteristics and power synthesis characteristics of array radiation transient electromagnetic pulse-based impulse radars [3]–[6], their respective physical significance remains highly controversial. Whether it is a frequency domain antenna array or a time domain antenna array, computation of key parameters still relies mainly on simulation with CST or HFSS software. However, for antenna arrays with large numbers of elements, such methods are not only time-consuming, but they are also inaccurate. For array impulse radars, timing and amplitude jitters triggered by impulse signal sources may cause serious impacts on system performance because such radars acquire target information that relies on the time or time difference information of echo signals. Thus, analytical analysis of time domain antenna arrays or fast numerical calculation has become a problem that requires an urgent resolution.

To solve the above problem, a time-difference-of-arrival(TDOA) method of target localization is proposed

that references the point source approximation method for frequency domain antennas by considering the elementary antenna as the radiation point source [7]–[12].

The time-difference-of-arrival(TDOA) method is widely used in wireless positioning, and has been used in cellular positioning system, WCDMA technology, wireless ranging radar, roadbed multi-point positioning and other positioning systems. Previous studies have introduced a lot of improvements and performance optimization of the time-difference-of-arrival(TDOA) method. In 2003, a paper explored the use of cross correlation based TDOA methods in conjunction with a novel technique for combining the time-difference-of-arrival(TDOA) estimates from multiple antenna pairs to build an estimate of the transmitter position [13]. Researchers proposed an improved time-difference-of-arrival(TDOA) localization scheme using PSO (Particle Swarm Optimization) in UWB (Ultra Wide Band) systems [14], [15]. The influence of the IEEE 802.15.4a channel model parameters on the performance of the time-difference-of-arrival(TDOA) localization method in Impulse Radio Ultra-Wide Band (IR UWB) systems was addressed [16]. IEEE 802.15.4a Ultra-wideband based wireless positioning has gained attention for precise localization. Researchers proposed and validated a novel approach for a multi-user time-difference of arrival based localization system using wireless clock synchronization [17]. Indoor localization with Uplink-Time -Difference-of-Arrival (U-TDOA) provided good scalability, high updates rates and high accuracy [18]. The specific challenge addressed in the paper is enabling novel applications with autonomous UAV systems through tight integration with scalable and precise receiver-side time-difference-of-arrival(TDOA) based ultra-wideband (UWB) indoor localization [19]. Researchers presented a time delay analysis for indoor localization based on time-difference-of-arrival(TDOA) algorithm, where they have performed both simulative and practical experiment together [20]. Finding the position of a radiative source based on time-difference-of-arrival (TDOA) measurements from spatially separated receivers has been widely applied in sonar, radar, mobile communications and sensor networks. The paper presents a weighted-least-squares (WLS) algorithm with the cone tangent plane constraint for hyperbolic positioning. The method adds the range between the source and the reference sensor as a dimension [21]. In order to improve the accuracy and engineering feasibility of four-Satellite localization system, the frequency difference measurement is introduced to the four-Satellite time-difference-of-arrival(TDOA) localization algorithm. The TDOA/FDOA (Frequency Difference of Arrival) localization algorithm is used to optimize the GDOP (geometric dilution of precision) of four-Satellite localization [22].

The above researches content are to improve and optimize the time-difference-of-arrival(TDOA) location method. In the paper, we've established a complete impulse system radar. By making use of target information extraction method in this paper through the time-domain array antenna equivalent to the point source approximation model, we've determined three positions of receiving the antenna in the time-domain array antenna and controlled the error of time-difference-of-arrival(TDOA) into a good scope through the deduction of mathematical formula. Through experiments and analyses, the approaches put forward in the paper have good prospects of application in the target positioning. The ultra wideband(UWB) technology is widely used in the positioning of the Internet of Things. The research in the paper is based on the ultra-wideband(UWB) technology. Therefore, the research results of the paper shall have a wide prospects of application in the positioning of the Internet of Things.

II. MATERIALS AND METHODS

A. POINT SOURCE APPROXIMATION

The elementary time domain antenna is equivalent to a point source of electromagnetic radiation. In the time-domain pattern, the function for radiation impulse signal waveforms remains the same. Radiation of an array time-domain antenna at a spatial point (r, θ, ϕ) can be calculated based on the wave superposition principle.

In Fig. 1, it is assumed that a planar array antenna has $m \times n$ numbers of array elements, the feed point coordinates of "i" numbered elementary antenna are $(x_i, y_i, 0)$, and the spatial coordinates of the target under detection are (x,y,z). Moreover, the distance between the target under detection and origin of coordinates is denoted by r, and r_i represents the distance between target under detection and the feed point of "i" numbered elementary antennas. However, calculation of array antenna parameters using the point source approximation model ignores the coupling effect between antenna elements. Three receiving antennas numbered ①, ②, ③, one transmitting antenna numbered ④.

B. TARGET LOCATION AND THE APPLICATION IN THE INTERNET OF THINGS

As shown in Fig. 1, for the target located at point (r, θ, ϕ), the time taken for its scattering echo signal to arrive at three or more non-collinear receiving antennas on the array plane differs. Utilizing this time difference, the target location can be determined. A receiving antenna is installed at the array plane center $(0,0,0)$. Supposing that the time difference from the feed time to the time at which the given antenna receives the target signal is t_{00} (in previous works, the feed time of this type of antenna is typically regarded as the starting time). Then, the radial distance of the target from the array plane center is

$$r = \frac{t_{00}c}{2} \tag{1}$$

After recording the t_{00} value, radial distance r of the target can be obtained by (1). Supposing that the time difference between the moment at which the "i" numbered receiving antenna receives the signal and the starting time is t_{i0}. Then, the radial distance r of the target detected by this antenna is

$$r = ct_{i0} - \sqrt{(x - x_i)^2 + (y - y_i)^2 + z^2} \tag{2}$$

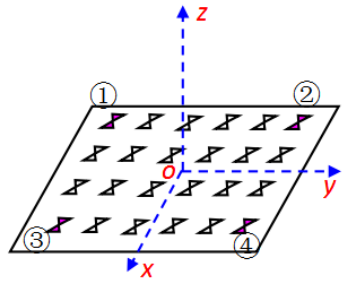

(a)

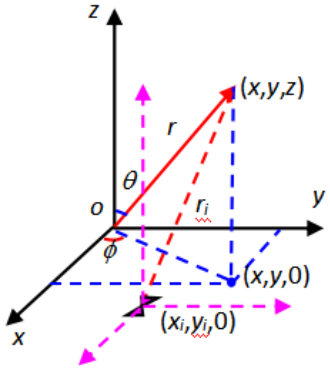

(b)

FIGURE 1. Point source approximation model.

According to (1), time difference t_{ij} in the reception of target signals between "i" and "j" numbered antennas is

$$\begin{cases} t_{ij} \equiv t_{i0} - t_{j0} = \dfrac{(\rho_i^2 - \rho_j^2) - 2r\rho_{ij}\sin\theta \cdot \sin\left(\phi + \gamma_{ij}\right)}{c(r_i + r_j)} \\ \rho_{ij} = \sqrt{(x_i - x_j)^2 + (y_i - y_j)^2} \\ \tan\gamma_{ij} = \dfrac{x_i - x_j}{y_i - y_j} \end{cases} \tag{3}$$

To facilitate the analytical solution of the target location coordinates (r, θ, ϕ), three receiving antennas numbered "① ", "②" and "③" in Fig. 1(a) are taken as the receiving antennas. As shown in Fig. 1(b), by selecting an antenna combination of "① + ③", we can obtain

$$x = \frac{rc}{l}t_{13} = \frac{t_{00}c^2}{2l}t_{13} \tag{4}$$

Where l is the side length of the square array antenna. Similarly, by selecting an antenna combination of "① + ②", we can obtain

$$y = \frac{rc}{l}t_{12} = \frac{t_{00}c^2}{2l}t_{12} \tag{5}$$

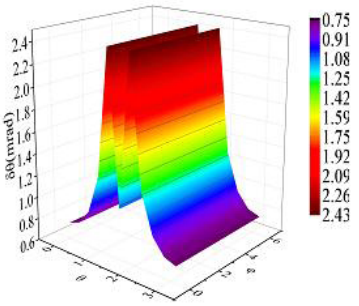

(a)

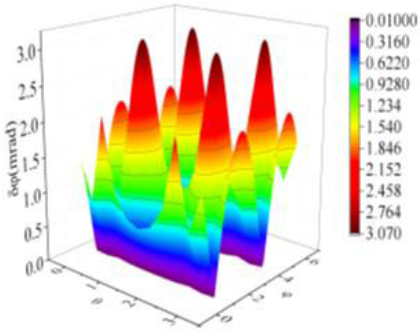

(b)

FIGURE 2. Angular error of TDOA method.

Thus, the target location coordinates are

$$\begin{cases} x = \dfrac{rc}{l}t_{13} = \dfrac{t_{00}c^2}{2l}t_{13} \\ y = \dfrac{rc}{l}t_{12} = \dfrac{t_{00}c^2}{2l}t_{12} \\ z = \dfrac{t_{00}c}{2l}\sqrt{l^2 - c^2(t_{12}^2 + t_{13}^2)} \end{cases} \tag{6}$$

In the above formula, t_{12} and t_{13} are calculated by (3);

$$\begin{cases} t_{12} = \dfrac{l}{c}\sin\theta \cdot \sin\phi \\ t_{13} = \dfrac{l}{c}\sin\theta \cdot \cos\phi \end{cases} \tag{7}$$

By transforming (6) into spherical coordinate system parameters, we obtain

$$\begin{cases} r = \dfrac{t_{00}c}{2l} \\ \theta = \arcsin\left[\dfrac{c}{l}\sqrt{t_{12}^2 + t_{13}^2}\right] \\ \phi = \arctan\left(\dfrac{t_{12}}{t_{13}}\right) \end{cases} \tag{8}$$

Any three non-collinear receiving antennas provide a location parameter (r, θ, ϕ) of the target. If there are n $(n \geq 3)$ number of receiving antennas, C_n^3 target locations are given. According to the conditions for minimization of the root-mean-square error for each location parameter, the minimally erroneous target location is obtained by fitting.

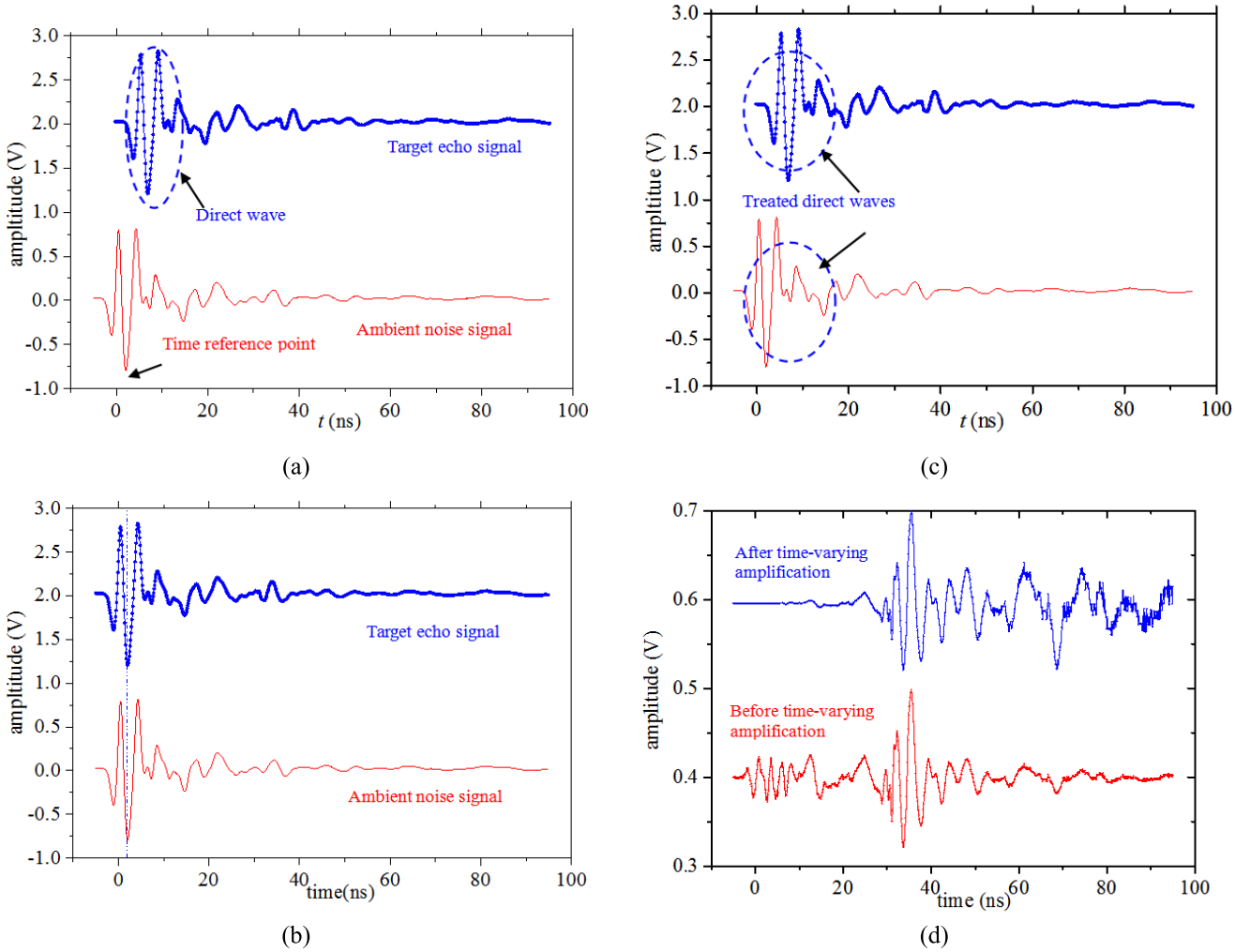

FIGURE 3. Comparison of data processing results before and after target information extraction.

The radial distance of the target is determined using (1) or (2). That is, the target image distance is determined by the time difference between the signal reception by each receiving antenna and the feed starting time. To determine the radial distance measurement error, (1) is totally differentiated to obtain

$$\delta r = \frac{c}{2}\delta t_{00} \tag{9}$$

Let $\delta t_{00} = 50$ ps, $\delta r = 7.5$ mm. Hence, the radial distance of the target is determined by the time difference between transmission and reception of signals by each receiving antenna, which has a centimeter-level accuracy.

By the total differential of the second formula in (8), angular localization accuracy can be obtained.

$$\delta\theta = \frac{c}{l \cdot \cos\theta} \frac{t_{12} \cdot \delta t_{12} + t_{13} \cdot \delta t_{13}}{\sqrt{t_{12}^2 + t_{13}^2}} \tag{10}$$

Considering that the signals received by the receiving antennas are collected by the same receiver, time jitters of the receiver can be considered to be approximately equal for different receiving antennas. That is, assuming that $t_{12} = \delta t_{13}$, then (10) can be simplified to

$$\delta\theta = \frac{c}{l \cdot \cos\theta} \frac{1}{\sqrt{1 - \frac{2t_{12}t_{13}}{(t_{12}+t_{13})}}} \delta t_{12} \tag{11}$$

When $r_i \gg \rho_i$, approximation $r_i + r_j \approx 2r$, *is* made, the first formula in (3) is simplified to

$$t_{ij} = \frac{-\rho_{ij} \sin\theta \cdot \sin\left(\phi + \gamma_{ij}\right)}{c} \tag{12}$$

When $\theta = k\pi$ or $\phi + \gamma_i = k\pi$, let $\delta t_{12} = \delta t_{13} = 5psl = 2$ m, then $\delta\theta = 0.75$ mrad. Figure 2(a) presents the θ angular localization error in any (θ, ϕ) direction under the above calculation conditions. The calculations reveal that the angular error provided by the TDOA localization method is around 2 mrad.

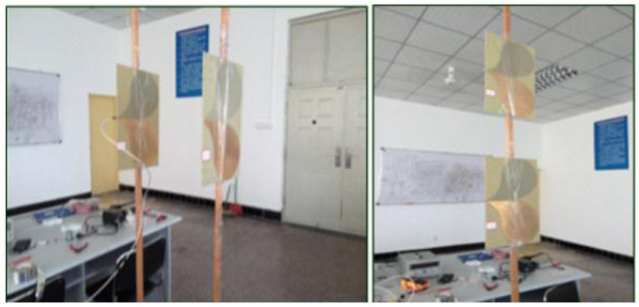

(a)

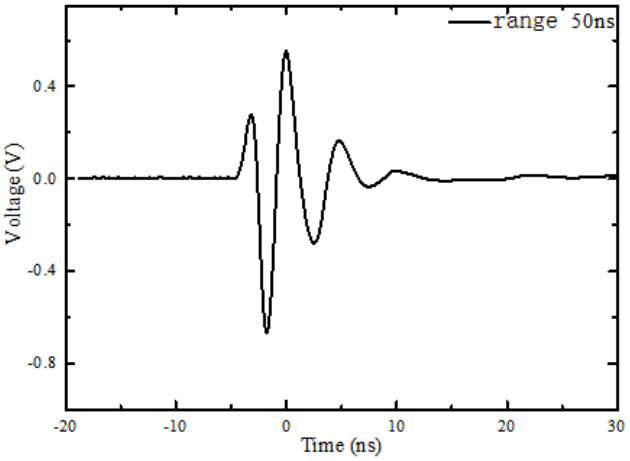

(c)

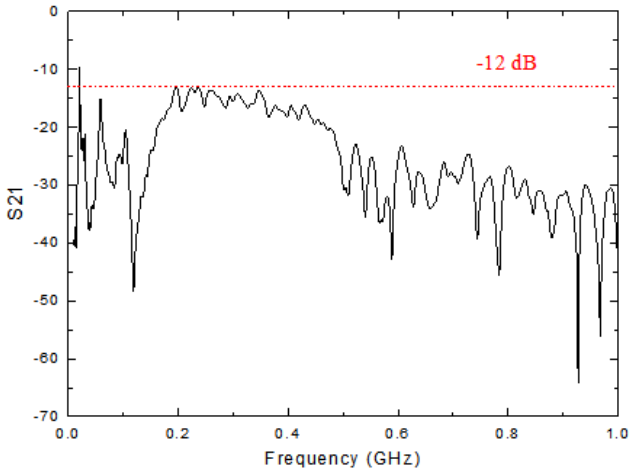

(b)

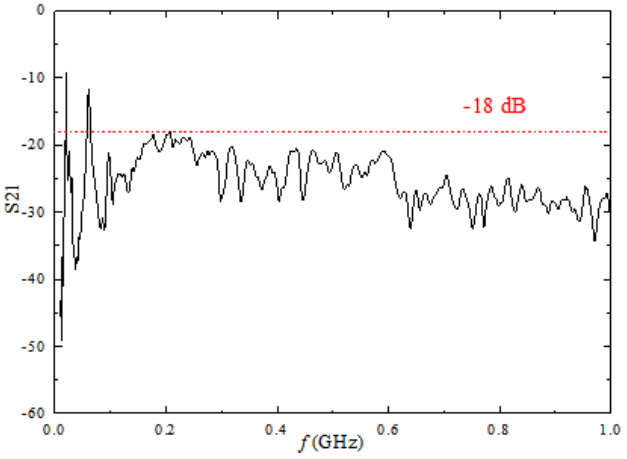

(d)

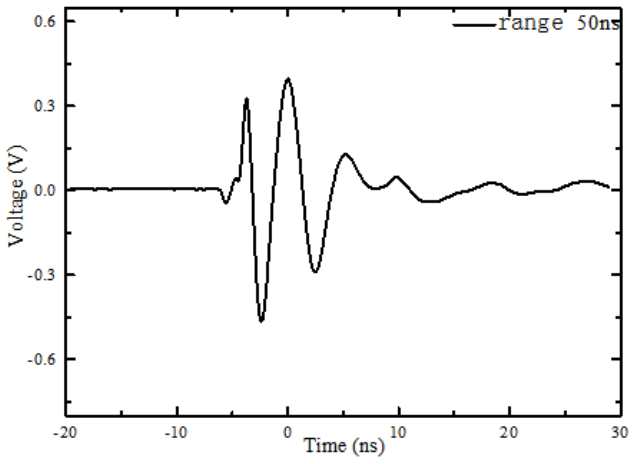

(e)

FIGURE 4. Experimental test results of coupling effect E and H planes for two-element antenna.

Similarly, by the total differential of the third formula in (8), angular localization accuracy can be obtained:

$$\delta\phi = \frac{\cos^2\theta\,(t_{13}-t_{12})}{t_{13}^2}\delta t_{12} = \frac{\cos^2\theta\cdot t_{23}}{t_{13}^2}\delta t_{12} \qquad (13)$$

Fig. 2(b) presents the angular localization error in any (θ, ϕ) direction under calculation conditions that are the same as in Fig. 2(a). Calculations reveal that the ϕ angular error provided by the TDOA localization method is around 3 mrad.

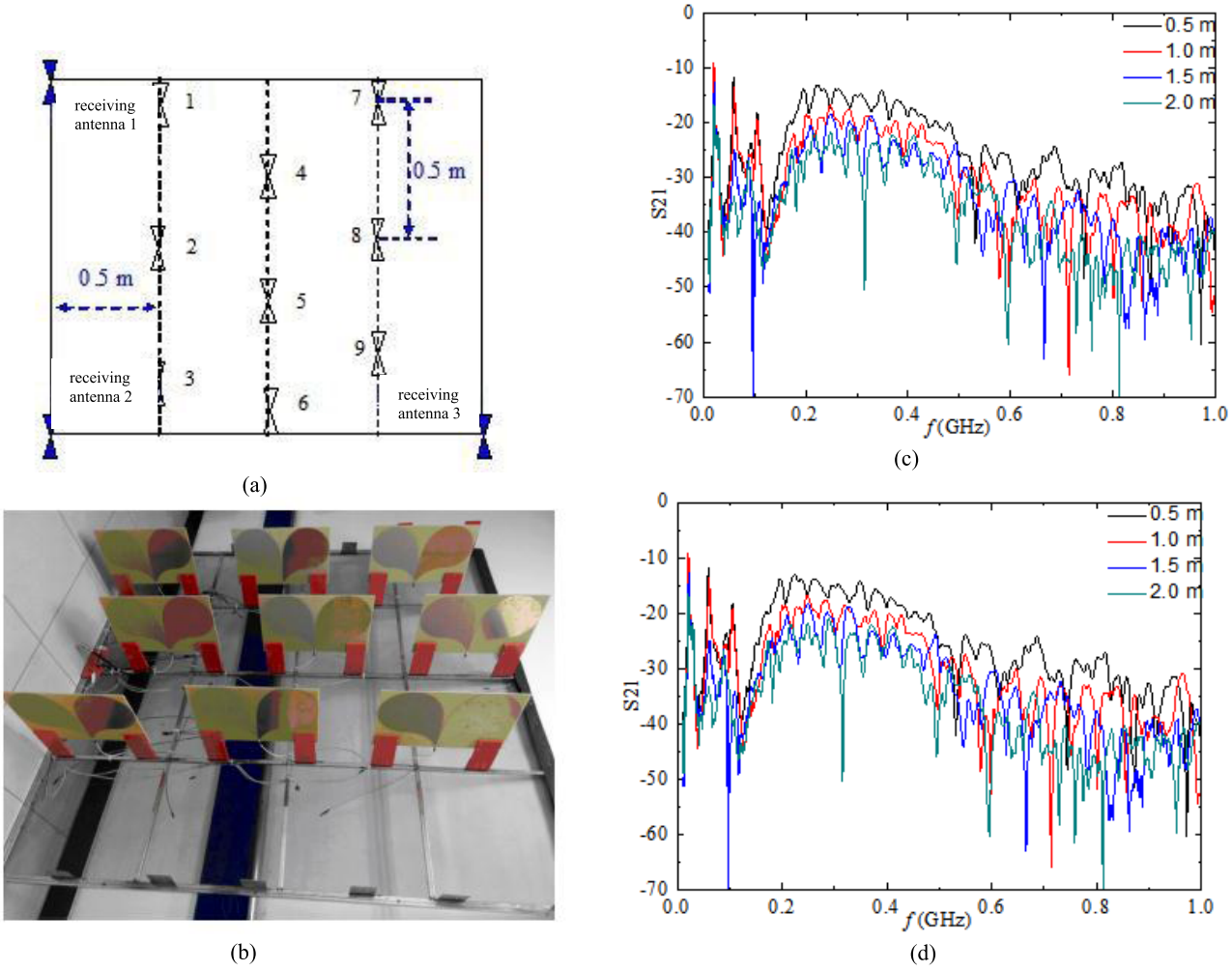

FIGURE 5. interleaving array antennas mode and array element antenna coupling.

The TDOA localization method is one of the localization technology in Internet of Things. The UWB indoor positioning technology often uses the TDOA demonstration location algorithm, which is a UWB system that carries out positioning according to the time difference of arrival of signals through hyperbolic crossover. It includes a radio system that generates, transmits, receives, and processes extremely narrow pulse signals. The UWB indoor positioning system includes a UWB receiver, UWB reference tags, and active UWB tags. In the process of positioning, the UWB receiver receives UWB signals transmitted by the tags. By filtering all kinds of noise interference in the transmission process of electromagnetic waves, the signals containing valid information are obtained, and calculation and analysis of location and distance measuring are conducted by the central processing unit. This article is to explore the application prospect of impulse radar in Internet of Things by studying the application of time-difference localization method in impulse radar.

C. TARGET INFORMATION EXTRACTION

In this section, we propose a simple method to extract target information by three steps time alignment, amplitude normalization, and time varying amplification and the corresponding data handler compilation method.

Figure 3(a) shows the signal curve detected by the impulse radar system depending on if the target is placed under the same experimental conditions. It can be observed that, in general, the target information is hidden in the environmental noise. The extraction of target information involves separating the echo information of target scattering from the intrinsic noise of the environment and radar system.

The impulse radar system adopts the time-domain waveform correlation reception method to detect the target. Combined with the working characteristics of the experimental prototype system developed in this paper, the radar system is initially stationary, and the ambient clutter remains unchanged for a short time. Secondly, the received signal is a time-domain signal, which is convenient to suppress and even

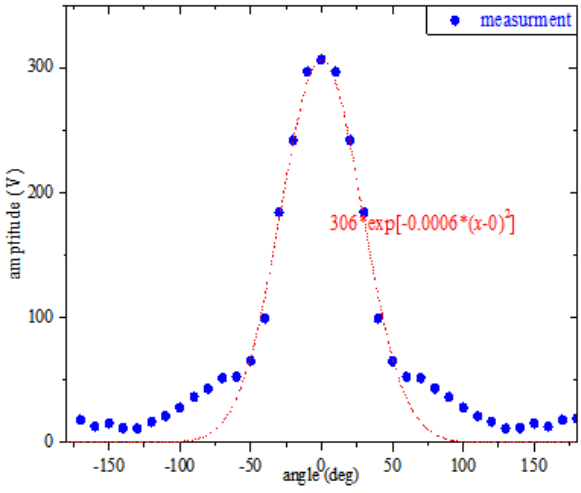

(a)

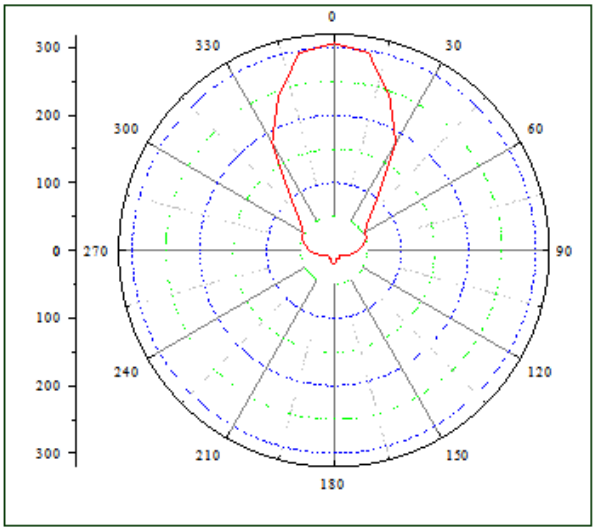

(b)

FIGURE 6. Experimental test of time-domain angular width central axis beam for antenna array.

eliminate the signal of random noise. Accordingly, we propose the following object information extraction method. Firstly, the characteristic point of the direct wave signal of the transmitting antenna and receiving antenna is used as the reference point of the starting point of the system timing. Secondly, environmental noise signal background is collected in advance. Thirdly, the environmental noise signal is removed from the echo signal containing the target information, and the effective information of the target is obtained.

III. EXPERIMENTAL TEST AND ANALYSIS

We used impulse radar with the following technical indices to perform experimental verification. Technical indices of impulse radar were as follows: number of array elements 3×3; array plane size 2×2 m^2; detection range (RCS $=$ 1 m^2) 1-2km; range resolution 0.3-0.5 m; array radiation power 80 kW; angular resolution 5°; repetition

(a)

(b)

FIGURE 7. Field experiment photo of array antenna.

frequency 5 kHz; beam scanning angle ±30°; angular scanning step 3°; and ambient temperature −40° − 80°.

Technical indices of elementary time domain antenna were as follows: center frequency 300 *MHz*; bandwidth 0.2-1 *GHz*; time-domain gain ≥2 *dB*; impedance 30-100 Ω; trailing signal/peak signal voltage ≤10:1; and time domain pattern (E-plane) 35°.

A. ARRAY METHOD, EXPERIMENTAL TEST AND ANALYSIS OF ARRAY TIME DOMAIN ANTENNAS

1. Experimental test and analysis of coupling effect between element antennas

Too wide time-domain pattern will increase the coupling effect between the adjacent element antennas, especially when the array beam needs scanning, the coupling effect between the earlier transmitting element antenna and the delayed transmission antenna is more obvious. The coupled time-domain waveforms of each unit antenna are carefully measured, which is of great significance to eliminate the inherent noise signal of the impulse radar system when the target echo signal information is extracted.

Fig. 4(b), (c) and Fig. 4(d), (e) show the experimental results of *S21* parameters and coupled time-domain waveforms when the antennas are placed in the left of Fig. 4(a) and the right of Fig. 4(a) respectively (1.62 m from the ground height and 0.6 m between the feeding points of the two antennas). The experimental results show that both S21 parameters

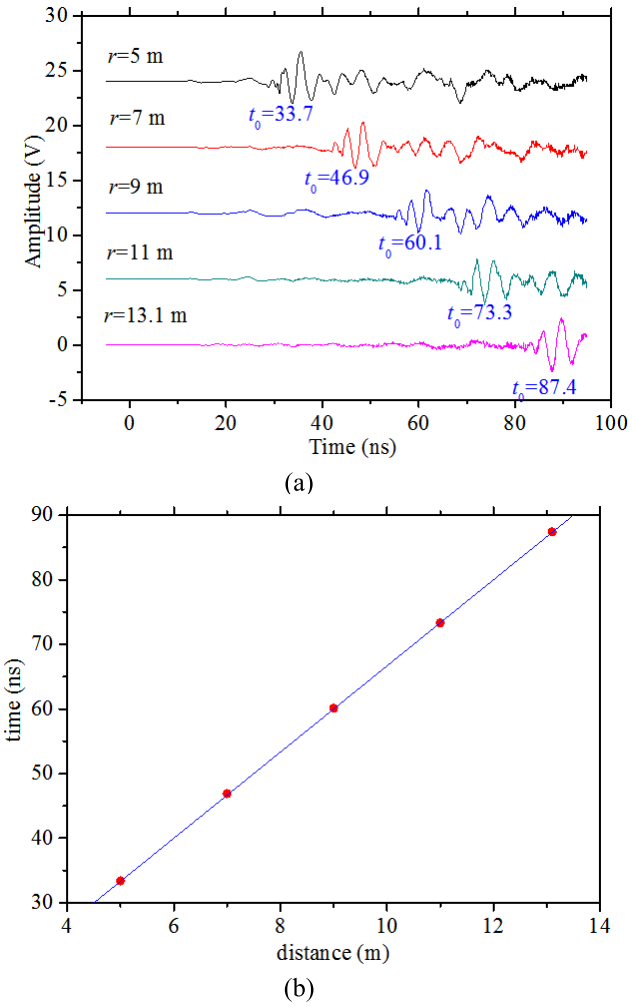

FIGURE 8. static target distance and range resolution test.

and coupled time-domain waveforms are more coupled than those placed along the E plane when the two antennas are placed along the H plane, which is easily explained by the wide time-domain pattern of the H plane of the element antenna.

Therefore, when considering the antenna array arrangement, we should avoid the H plane alignment of adjacent antennas as much as possible (the left of Fig. 4(a)).

Based on the pattern of the element antenna and the influence factors of the coupling effect between adjacent antennas, the experimental test and analysis are carried out. Fig. 5(a) and Fig. 5(b) show the interleaving array of the antenna elements (including the position of the radiation antenna and the receiving antenna) and the physical photographs of the antenna surface respectively. Of course, it is not possible to reduce the coupling effect between adjacent antennas by the method of interleaving array because the time-domain pattern of the H-plane the element antenna exceeds (60°). Fig. 5(c) and (d) show the variation trend of the coupling effect weakened when the *S21* parameters between adjacent antennas and the distance increased.

It can be seen that the coupling effect of interleaving array adjacent antennas is weaker than that in the left of Fig. 4(a) array. With the increase of the distance between adjacent antennas, the coupling effect gradually weakens, but it is not realistic to reduce the coupling effect between the elements by increasing the aperture of the array surface or the spacing between the adjacent element antennas.

B. EXPERIMENTAL TEST AND ANALYSIS OF ANTENNA ARRAY SURFACE BEAM ANGLE

Figs. 6 show the experimental results (solid points) and the fitting function (dashed lines) of the antenna array surface radiation beam E surface in time-domain pattern when it is on the central axis. In the experiment, the center of the transceiver antenna is 2.8 m from the ground height and the distance between the transceiver antenna is 12 m.

The fitting function in the Fig. 6 (a) is

$$\Theta(\theta) = \theta_0 \cdot \exp\left(-0.0006 \cdot \theta^2\right) \tag{14}$$

According to the (14) formula, the half-angle width of the array plane beam can be obtained.

$$\delta = \sqrt{\frac{4\ln(2)}{0.0006}}\frac{1}{2} = 33.99^\circ \tag{15}$$

The experimental results show that: first, the time-domain pattern of the element or array antenna can be expressed by Gaussian function approximation, that is, the Gaussian function approximation is reasonable; Second, the array beam width is about 34° , which is approximately equal to the half angle width (35°) of the half peak amplitude of the element antenna.

C. TEST AND ANALYSIS OF TARGET DISTANCE DETECTION EXPERIMENT

Under static condition, the target distance test device is shown in Fig. 7. The experiment uses a single receiving antenna to receive the target echo signal, and the experimental conditions of the transmitting antenna array surface from ground height parameter Fig. 4 show that the receiving antenna is located in the center of the radiation array surface.

Fig. 8(a) shows the experimental test results of the target echo information obtained by using the target information extraction method introduced in Section II. When the target is placed at 5-13.1 m different distance points from the radiation array surface, respectively. Table 1 shows the difference between the experimental test results shown in Fig. 8(b) and the theoretical calculation values.

The Table 1 comparison results between the experimental test and theoretical calculation show that the accuracy of the distance measurement of the impulse radar can reach the order of centimeters.

D. EXPERIMENTAL TEST AND ANALYSIS OF TARGET RANGE RESOLUTION

The target radial range resolution radar system was measured on two targets within easy reach of the radial

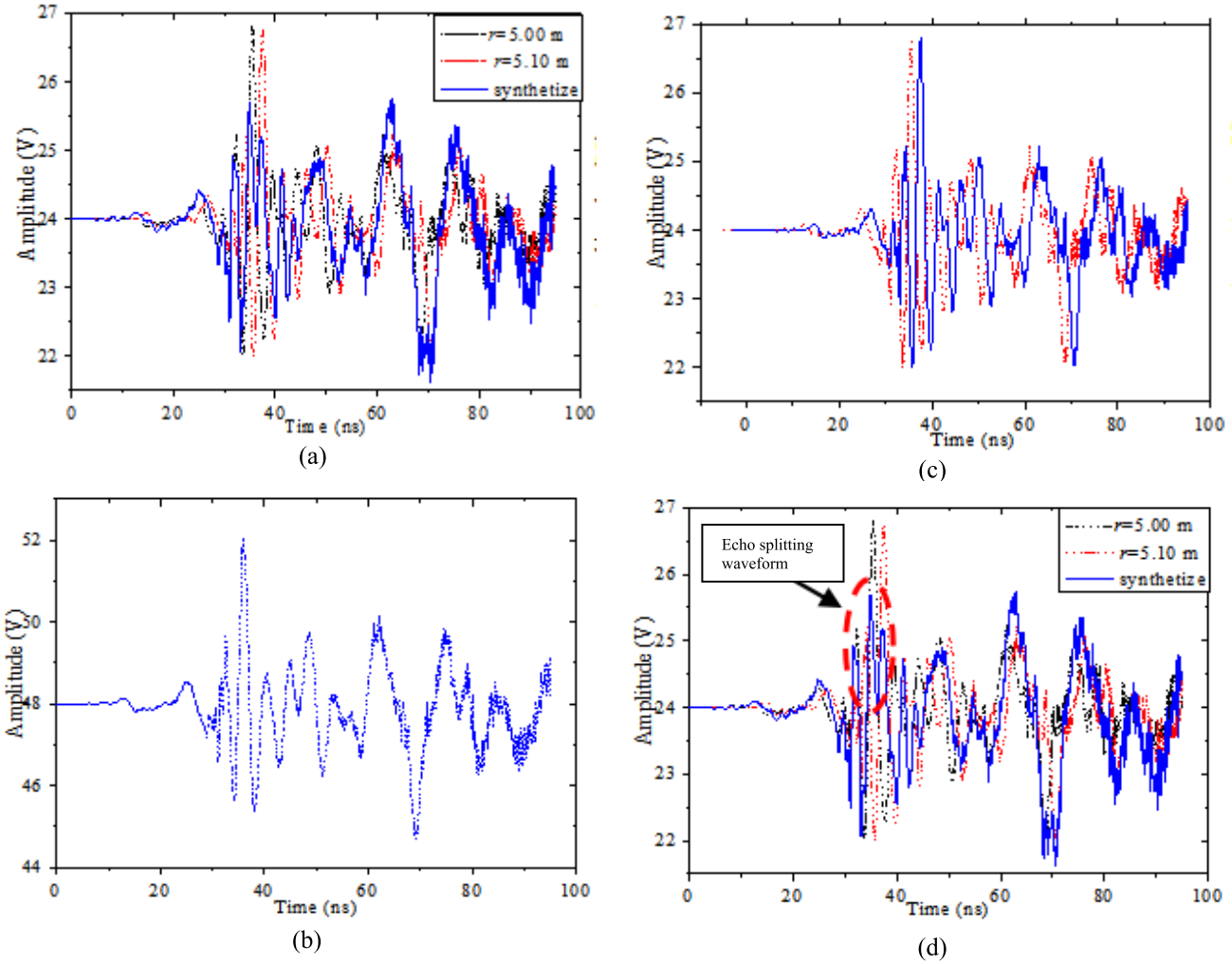

FIGURE 9. target distance resolution test.

TABLE 1. Comparison between experimental and theoretical calculation of static target distance.

The target distance	*Theoretical echo time (ns)*	*Test echo time (ns)*	*Echo time error (ns)*	*Distance test error (cm)*
5m	*33.6*	*33.7*	*0.1*	*1.5*
7m	*46.7*	*46.9*	*0.2*	*3*
9m	*60.0*	*60.1*	*0.1*	*1.5*
11m	*73.3*	*73.3*	*0*	*0*
13.1m	*87.3*	*87.4*	*0.1*	*1.5*

(multi-objective) or identification ability. It was composed of target echo signal peaks, and troughs distinguished the two echo signals.

In the experimental test, two single objectives were measured in a smaller distance (such as the distance of 10 cm) of the target signal. We measured the target echo signal, and examined whether the double target echo signal peaks and troughs distinguished the two impulse signals to determine the radial range resolution of the system.

Fig. 9(a) shows the target signal received by the prototype system when the distance between two single targets from antenna the array surface is 5 m and 5.15 m, respectively. Fig. 9(b) shows the target echo information when two objects are placed 5 m and 5.15 m away from the antenna array surface, respectively. Figs. 9(c) and (d) show the increased radial distance difference between the two targets to 30 cm. We repeated the experiment. The results are shown in Figs. 9(a) and (b). The experimental test conditions are the same as those in Fig. 8.

In Fig. 9(b), the experimental test results show that the two target echo signals are 15 cm apart. The pulse width of one is obviously wider than the single target echo signal, However, there is only one wave. The two goals are system testing for a single objective. When the spacing of the two

TABLE 2. Transceiver antenna coordinates for target azimuth test.

The antenna number	*Transmitting antenna*	*Receiving antenna 1*	*Receiving antenna 2*	*Receiving antenna 3*
Position coordinate (m)	*(0,0)*	*(-1,-1)*	*(-1,1)*	*(1,-1)*

targets increases to 30 cm, as shown in Fig. 9(d), the dual target echo signal wave obviously divides into two. The pulse width is close to twice the single target echo signal. A radar system at this time can distinguish targets. Considering that the semi-peak width of the radiation pulse signal in the experimental prototype system is 2 ns, the radial distance resolution is 30cm, which is consistent with the experimental test results in Fig. 9(d). Thus, the conclusion that the distance resolution of the impulse radar is determined by the Rayleigh criterion, which can be recognized by the dual-pulse being experimentally verified.

E. EXPERIMENTAL TEST AND ANALYSIS OF TARGET ANGULAR RESOLUTION

The general multi-objective radial distance or distance by their time of echo signal to determine, but when multiple target distance equidistant from the radiation front, and the azimuth Angle (θ, ϕ) not phase at the same time, the target echo signal to radiation on the surface of the array is almost the same time, not by a single receiving antenna to receive different time to determine the target. In frequency domain radar, usually according to different location target for position in the front beam Angle is different, so the differences of echo signal amplitude, by analyzing the amplitude difference of different target to determine the target azimuth. Considering that the time can accurately measure the impulse signal (as shown in Fig. 8 and Fig. 9 experimental test results), we propose the multiple antenna signal time to determine the target coordinates or azimuth.

During the experiment, the three receivers were exposed to the antenna at the center of the antenna, and the three receiving antennas received the target echo. The three receiving antennas are shown in Fig.1(a), and the coordinates of the location are given in Table 2. Other experimental test conditions are the same as those in Fig. 8

The waveform curves of the target echo signals received by the three receiving antennas are similar to those shown in Fig. 8(a). Waveform graphs of the experimental test are not listed here owing to space constraints. Only the position coordinates of the target placement are listed in Table 3, where Antenna I delay refers to the first I number target information and the receiving antenna receives the direct plot of the timing starting point in time (the unit is ns). We refer to the goal of target location coordinates (r, θ, ϕ), among them. The unit of the distance coordinate is m, and the angle coordinate unit is Degree.

TABLE 3. Test results and analysis of target azimuth experiment.

Receiving antenna delay (ns)			*Actual placement coordinates of the target*			*Experimental test coordinates of the target*		
antenna 1	*antenna 1*	*antenna 1*	r	θ	Φ	r	θ	Φ
62.280	*62.295*	*62.273*	*10*	*0*	*0*	*10.09*	*0.15*	*85.95*
65.440	*62.290*	*62.285*	*10*	*45*	*45*	*10.35*	*42.4*	*44.9*
65.325	*63.120*	*61.410*	*10*	*45*	*30*	*10.37*	*42.4*	*29.9*
131.020	*129.390*	*128.171*	*20*	*30*	*30*	*20.27*	*29.5*	*29.80*

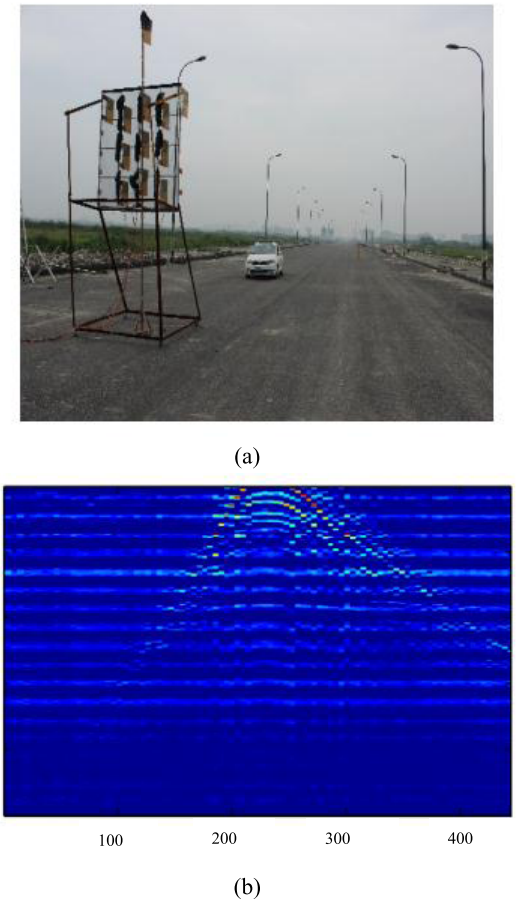

(a)

(b)

FIGURE 10. Experimental site photos of single moving target and imaging results.

Table 3 experimental results show that the accuracy of the radial distance measurement of the impulse radar can be maintained within a 0.5 m range. Secondly, when the target is placed in some special position, such as (10, 0, 0),

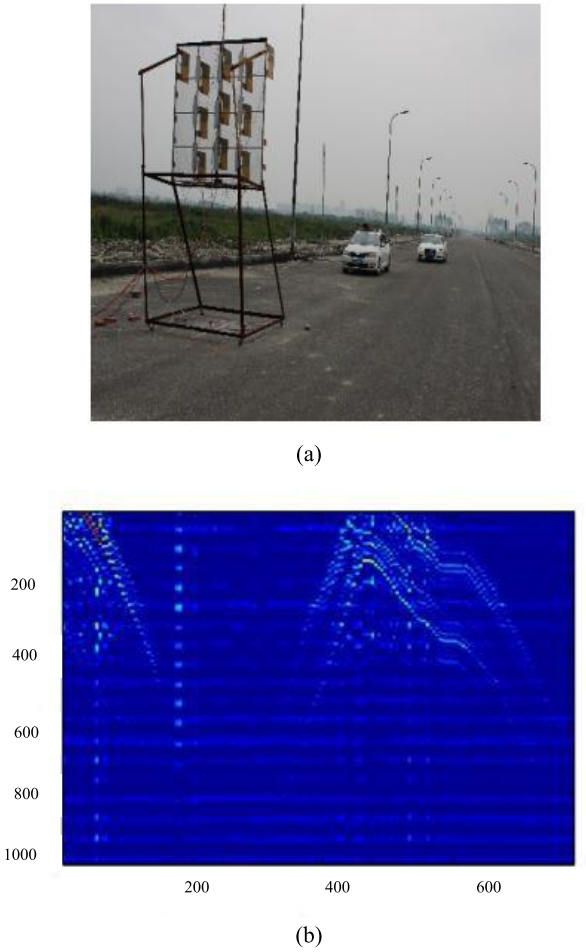

FIGURE 11. Experimental site photos of two moving targets and imaging results.

the azimuth deviation is large (such as putting the target on the axis). Thirdly, within the scope of the scanning angle, and the target placed in a special angle, the jet lag positioning method can accurately locate the target bearing. The angular position error can guarantee the mrad magnitude; The theoretical analysis results are given in Section II.

The error of the experimental data in Table 3 is still close to the result of the Section II analytical analysis because, in the analysis, the system impulse triggering jitter is set to 5 ps; however, the system jitter is on the order of 10 ps. Secondly, in the experimental data processing, the application directly reads the direct wave signal feature point of time, not to direct wave signal waveform curve formula proposed merger to read its feature point time, cause the system to trigger jitter (about 30-50 ps) included in the orientation parameter values directly, greatly enhance the error. Therefore, it includes further reducing the trigger jitter error caused by the system hardware from the hardware, further increasing the number of receiving antennas, optimizing the program of time difference positioning algorithm, and improving the target positioning algorithm.

F. DYNAMIC TARGET

The experimental site for a single moving target is designed as shown in Fig. 10(a). The impulse signal is radiated using a 3×3 elementary array. The receiving antenna is fixed on the array plane of the sending antenna, which is directly above the radiation array plane. The detection target is a moving vehicle. During the experiment, the car moves from far to near or from near to far at velocities varying within 60 km/h. Fig. 8(b) presents the grayscale image provided by imaging software when the car moves from far to near. As can be observed, the impulse radar system introduced in this paper achieves imaging of moving targets.

The conditions and methods for double moving target imaging experiments were the same as the corresponding single target experiment. During the experiment, two moving cars were tested separately under parallel and front-back running scenarios. The experimental site and typical results are shown in Fig. 11. Fig. 11(b) clearly shows two movement curves of the two cars. Moreover, deceleration and pause information of the two cars during movement are also clearly displayed. This not only indicates that the impulse radar system achieves clear imaging of two or more moving targets, but it also provides experimental evidence that the prototype system has a good angular resolution.

IV. CONCLUSION

In the frequency domain array radar, usually radar antenna beam parameters are employed. The target echo signal amplitude and goal orientation often require repeating many times the same target detection and calculation method. Complex precision is also limited, especially for some quick target positioning. The e limitations of the method hence become more obvious.

Considering that the time-domain radar mainly relies on the time or time difference of the target echo signal to complete the target detection, and the time difference measurement accuracy of a commercial chip reaches 10 ps, the time difference of the target echo signal of the non-collinear multi-antenna (three or more) was addressed in Section II. The time difference localization method of the target positioning was adopted. According to the experimental results of the target detection of the prototype system in Section III, the method of time difference localization can locate the target accurately.

According to characteristics such as obvious characteristic points of direct wave coupling between antennas in the array receiving and the sending time domain, small environmental interference, easy fitting, and known waveform curve functions, we proposed a direct wave signal as a reference signal. The method selects the signal to obtain the timing of the signature, which is the time calibration and amplitude of the time calibration to the echo of the target information and ambient noise. The target echo signal after time calibration and amplitude normalization is subtracted from the environmental noise signal to obtain the target information. On this basis, the time-varying amplification processing is carried out

for each time-point data signal of the target information to obtain clear target information. In Section IV, the experimental test and analysis of the data processing of the target echo signal shows that the approach based on the above method can obtain clearer images of the static and dynamic targets.

UWB positioning technology is a very important part of the Internet of things location technology. UWB can be used for precise indoor positioning, for example, position detection of battlefield soldiers, robot motion tracking, and so on. Compared with conventional narrowband systems, the UWB system has the advantages of strong penetration capability, low power consumption, excellent anti-interference effect, high security, low system complexity, and precision positioning. Therefore, the UWB technology can be used to locate, track and navigate indoor stationary or moving objects and people, and can provide a very good positioning accuracy. The accuracy can be maintained between 0.1m $\sim$ 0.5m depending on the technical means or algorithms used by different companies. It can be seen that this technology studied in this article has broad application prospects in the future development of Internet of Things.

REFERENCES

[1] G. M. Loubriel *et al.*, "Optically-activated GaAs switches for ground penetrating radar and firing set applications," in *Proc. 12th IEEE Int. Pulsed Power Conf.*, vol. 2, Jun. 1999, pp. 673–676.

[2] E. E. Funk and C. H. Lee, "Free-space power combining and beam steering of ultra-wideband radiation using an array of laser-triggered antennas," *IEEE Trans. Microw. Theory Techn.*, vol. 44, no. 11, pp. 2039–2044, Nov. 1996.

[3] T. T. Wu, "Electromagnetic missiles," *J. Appl. Phys.*, vol. 57, no. 7, p. 2370, 1985.

[4] G. Wang, W. B. Wang, and C. H. Liang, "Beam characteristics of short-pulse radiation with electromagnetic missile effect," *J. Appl. Phys.*, vol. 83, no. 10, p. 5040, 1998.

[5] J. M. Myers, H. M. Shen, and T. T. Wu, "Curved electromagnetic missiles," *J. Appl. Phys.*, vol. 65, no. 7, pp. 2604–2610, 1989.

[6] Y. hongchun, R. Chengli, and L. weitao, "Beam scanning and decaying property of linear element planar antenna array," *Chin. J. Radio Sci.*, vol. 18, no. 5, pp. 496–501, 2003.

[7] H. Shi, H. Zhang, and X. Wang, "A TDOA technique with super-resolution based on the volume cross-correlation function," *IEEE Signal Process. Soc.*, vol. 64, no. 21, pp. 5682–5695, Nov. 2016.

[8] H. Yang and J. Chun, "An improved algebraic solution for moving target localization in noncoherent MIMO radar systems," *IEEE Trans. Signal Process.*, vol. 64, no. 1, pp. 258–270, Jan. 2016.

[9] S. Bartoletti, A. Giorgetti, M. Z. Win, and A. Conti, "Blind selection of representative observations for sensor radar networks," *IEEE Trans. Veh. Technol.*, vol. 64, no. 4, pp. 1388–1400, Apr. 2015.

[10] B. Vo and W. Ma, "The Gaussian mixture probability hypothesis density filter," *IEEE Trans. Signal Process.*, vol. 54, no. 11, pp. 4091–4104, Nov. 2010.

[11] J. Li, H. Pang, F. Guo, L. Yang, and W. Jiang, "Localization of multiple disjoint sources with prior knowledge on source locations in the presence of sensor location errors," *Digit. Signal Process.*, vol. 40, pp. 181–197, May 2015.

[12] T. Abrudan, Z. Xiao, A. Markham, and N. Trigoni, "Distortion rejecting magneto-inductive 3-D localization (MagLoc)," *IEEE J. Sel. Areas Commun..*, vol. 33, no. 11, pp. 2404–2417, May 2015.

[13] D. Young, C. Keller, D. Bliss, and K. Forsythe, "Ultra-wideband (UWB) transmitter location using time difference of arrival (TDOA) techniques," in *Proc. Conf. Signals, Syst. Comput.*, 2003, vol. 2, no. 2, pp. 1225–1229.

[14] T. Le, J. Kim, and Y. Shin, "An improved TDoA localization with particle swarm optimization in UWB systems," *J. Korean Inst. Commun. Inf. Sci.*, vol. 35, no. 1c, pp. 87–95, 2010.

[15] T. Le, J. Kim, and Y. Shin, "TDoA localization based on particle swarm optimization in UWB systems," *IEICE Trans. Commun.*, vol. 94, no. 7, pp. 2013–2021, Jul. 2011.

[16] J. Kaitovic and M. Eric, "TDOA localization in ir UWB systems," in *Proc. Int. Conf. Syst.*, 2011, pp. 118–121.

[17] J. Tiemann, F. Eckermann, and C. Wietfeld, "ATLAS—An open-source TDOA-based ultra-wideband localization system," in *Proc. Int. Conf. Indoor Positioning Indoor Navigat.*, 2016, pp. 1–6.

[18] S. Leugner, M. Pelka, and H. Hellbrück, "Comparison of wired and wireless synchronization with clock drift compensation suited for U-TDoA localization," in *Proc. Positioning, Navigat. Commun.*, 2017, pp. 1–4.

[19] J. Tiemann and C. Wietfeld, "Scalable and precise multi-UAV indoor navigation using TDOA-based UWB localization," in *Proc. Int. Conf. Indoor Positioning Indoor Navigat.*, 2017, pp. 1–7.

[20] B. Barua, N. Zaarour, N. Hakem, and N. Kandil, "Effect of UWB channel time delay parameters on TDOA localization," in *Proc. 6th Int. Conf. Digit. Inf., Netw., Wireless Commun. (DINWC)*, 2018, pp. 32–36.

[21] B. Jin, X. Xu, and T. Zhang, "Robust time-difference-of-arrival (TDOA) localization using weighted least squares with cone tangent plane constraint," *Sensors*, vol. 18, no. 3, p. 778, 2018.

[22] X. Guo, Y. Zhang, and B. Zeng, "Passive localization using time difference of arrival and frequency difference of ArrivalWC," *J. Comput. Commun.*, vol. 06, no. 1, pp. 65–73, 2018.

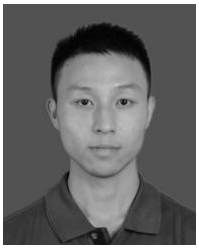

LONGFEI DANG received the B.Sc. and M.Sc. degrees in applied mathematics from the Chengdu University of Information Technology, China, in 2010 and 2013, respectively. He is currently pursuing the Ph.D. degree in condensed matter physics with the School of Physics, University of Electronic Science and Technology of China. His research interests include time-domain antenna, impulse signal, radar system, and imaging of time-domain radar.

HONGCHUN YANG received the B.Sc. degree in physics from Sichuan Normal University in 1989, the M.Sc. degree in field theory and particle physics from Sichuan University in 1997, and the Ph.D. degree in electromagnetic field and microwave technology from the University of Electronic Science and Technology of China in 2008. Since 1997, he has been a Teacher with the School of Physics, University of Electronic Science and Technology of China. He is involved in ultra-wideband radar (UWB) signal source, UWB antenna, UWB radar system and application, complex electromagnetic environment and complex network research.

BAOHUA TENG received the B.Sc. degree in physics from Hohai University in 1982, the M.Sc. degree in physics from Xi'an Jiaotong University in 1986, and the Ph.D. degree from Sichuan University in 2002. Since 2005, he has been a Professor with the School of Physics, University of Electronic Science and Technology of China. He is involved in condensed matter physics, theoretical physics, and quantum computation.